Orthopaedics & Traumatology: Surgery & Research 105 (2019) 291–299

Contents lists available at ScienceDirect

Orthopaedics & Traumatology: Surgery & Research

journal homepage: www.elsevier.com

Original article

Can objective criteria for poor tolerance of proximal humerus malunion be identified?

Aude Griffart[a,*], Pauline Joly-Monrigal[b], Julien Andrin[b], Cyril Lazerges[b], Michel Chammas[b], Bertrand Coulet[b]

[a] *Service de chirurgie orthopédique, hôpital de La Cavale Blanche, CHU, boulevard Tanguy-Prigent, 29200 Brest cedex, France*
[b] *Service de chirurgie de la main et du membre supérieur, chirurgie des nerfs périphériques, hôpital Lapeyronie, CHU, 371, avenue du doyen Gaston-Giraud, 34000 Montpellier cedex, France*

ARTICLE INFO

Article history:
Received 9 February 2018
Accepted 5 November 2018

Keywords:
Malunion
Shoulder
Fractures
Interobserver reliability: Intraobserver reproducibility: Computed tomography

ABSTRACT

Background: Malunion of the proximal humerus is common and variably tolerated. Classifications developed for proximal humerus malunion (PHM) rely on standard radiographs, which underestimate bone fragment displacement and lack accuracy. The clinical tolerance of PHM is subjective, and revision surgery is not always necessary. The primary objective of this study was to assess the reproducibility and relevance of four CT angle measurements for objectively quantifying the morphological disharmony caused by PHM in a control population then in a population with PHM. The secondary objectives were to identify angle cut-offs and to assess the correlations between angle values and the clinical tolerance of PHM.
Hypothesis: Objective criteria for assessing proximal humerus malunion can be identified using CT scans.
Materials and methods: Four angles were chosen to quantify proximal humerus disharmony: the angles between the humeral head and the glenoid in the coronal plane (HGCo) and axial plane (HGAx), the angle of tuberosity divergence in the axial plane (TDAx), and the centrum collum diaphyseal angle (CCD). The reproducibility of measurements of the four angles on computed tomography (CT) views was evaluated in a control population and in 46 patients with PHM. To this end, the reproducibility of reference slice selection was determined and intra- and interobserver reproducibility of the angle measurements was then assessed. Patients with PHM were divided into two groups based on clinical tolerance to allow testing for disharmony parameters associated with poor clinical tolerance, which was defined as functional impairment and surgical revision.
Results: Slice selection was found to be reproducible. The Bland-Altman plot indicated that the angle measurements in both the controls and the patients were reproducible within ±2 SDs. Intraclass correlation coefficient values ranged from fair to excellent for all angles in both the controls and the patients. The mean TDAx was higher in the patients than in the controls (72.0° vs. 56.1°, $P < 0.05$) and, within the PHM group, was higher in the subgroup with good vs. poor clinical tolerance (75.8° vs. 69.5°, $P < 0.05$). The CCD angle was greater in the controls than in the patients (129.8° [range, 128.3°–131.3°] vs. 125.9° [range, 122.9°–128.9], respectively) and was significantly greater in the PHM subgroup with good vs poor clinical tolerance (131.4° vs. 122.3°, respectively; $P = 0.007$). The HGCo and HGAx angles were significantly greater in the patients than in the controls (HGCo: 66.6° vs. 52.2°, respectively; HGAx: 17.5° vs. 13.3°, respectively, $P = 0.55$).
Discussion: The measurement method described here provides a quantitative assessment of postfracture disharmony based on four angles, the HGCo, HGAx, and TDAx. Measurement of these four angles on CT images was found to have good intra- and interobserver reproducibility. The angle values were significantly greater in the patients with PHM than in the controls. Within the patient group, the subgroup with poor clinical tolerance had smaller values of the TDAx, CCD, and HGAx angles and a greater value of the HGCo angle.
Level of evidence: IV, retrospective observational study.

* Corresponding author.
E-mail address: audegriff@hotmail.com (A. Griffart).

https://doi.org/10.1016/j.otsr.2018.11.020
1877-0568/

1. Introduction

Proximal humerus fractures are common, with an incidence rate of 246/100,000 population [1], and can result in malunion. Restoring the normal shoulder anatomy is essential to optimise the functional outcome [2,3]. Proximal humerus malunion (PHM) may be related to inadequate initial reduction or to secondary displacement [2,4–5] after non-operative treatment (22–80%) or after surgery (20–35%) [6–8]. PHM, defined as bone healing in a non-anatomical position, can cause pain and motion-range restriction. Perfect anatomical reduction of proximal humerus fractures is rarely achieved. However, PHM may be well tolerated, making surgical revision unnecessary. Tolerance depends on the degree of disharmony among the tuberosities, humeral head, and glenoid.

Available classifications for PHM rely on radiographs [7–9]. The most widely used, developed by Boileau et al. [9], provides useful therapeutic guidance but fails to assess the factors that govern the clinical tolerance of PHM. The evaluation on standard radiographs of displacements of the tuberosities, humeral head, and glenoid is not only challenging, but also lacks accuracy, notably due to underestimation of tuberosity malposition in the axial plane [2,7]. Computed tomography (CT) with or without contrast injection and 3D reconstructions is now considered indispensable to the evaluation of shoulder fractures and PHM [2,3,6,10,11,12]. The components of PHM are the greater and lesser tuberosities, humeral head, and glenoid. To the best of our knowledge, no validated methods for obtaining objective CT measurements of these parameters have been published. In addition, the disharmony cut-off above which PHM is poorly tolerated is unknown.

The primary objective of this study was to assess the reproducibility and relevance of four CT angle measurements for objectively quantifying the morphological disharmony caused by PHM in a control population then in a population with PHM. The secondary objectives were to identify angle cut-offs and to assess the correlations between angle values and the clinical tolerance of PHM. The working hypothesis was that objective criteria for assessing proximal humerus malunion could be identified using CT scans.

2. Materials and methods

2.1. Study population

2.1.1. Controls

The control group was a random sample of 30 consecutive CT or CT-arthrography scans of normal shoulders in adults with no history of shoulder surgery, instability, or laxity. Individuals at risk for having lesions of the glenoid and/or humeral bone, capsule, and/or ligaments were not eligible as controls.

2.1.2. Patients with malunion

We retrospectively identified 61 patients managed at our department for PHM since 2000 (Fig. 1). PHM was defined as the presence of at least one of the following radiological criteria [2,9]: postero-superior displacement of the greater tuberosity along more than 1 cm, medial displacement of the lesser tuberosity along more than 1 cm, and a central collum diaphyseal (CCD) angle smaller than 120° or greater than 140°. The presence or absence of avascular necrosis of the humeral head with or without a necrotic sequester was recorded. Displacement of the tuberosities relative to their normal position was evaluated on coronal and sagittal CT views for the greater tuberosity and on the axial CT view for the lesser tuberosity. The distance between tuberosity position on the CT views and the anatomical position was measured in centimetres. The CCD angle was measured on a coronal CT view.

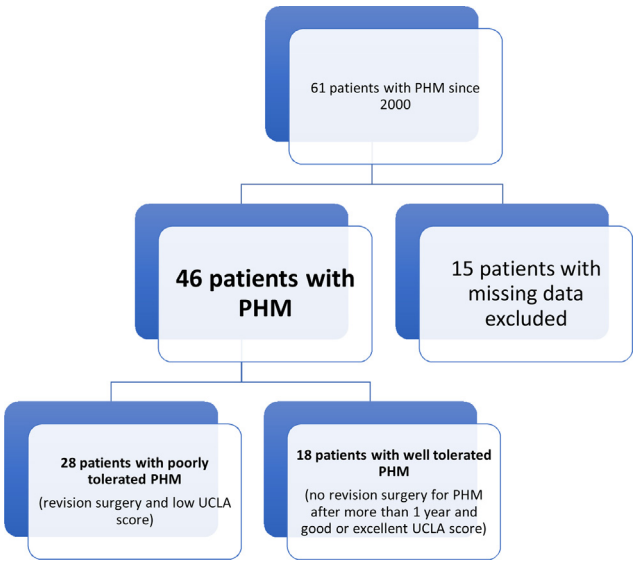

Fig. 1. Flow diagram of the patients with proximal humerus malunion (PHM).

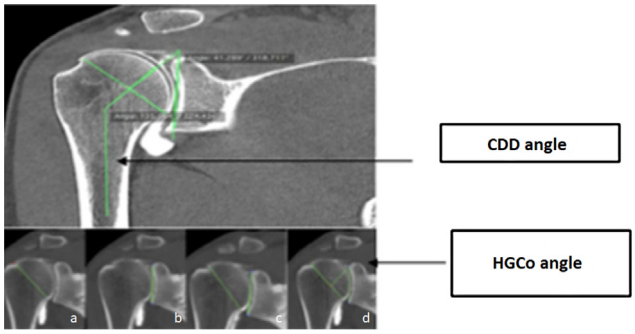

Fig. 2. Coronal view: measurement of the centrum collum diaphyseal (CCD) angle and of the angle subtended by the axes of the humeral head and glenoid (HGCo). a) humeral head axis drawn between the superior and inferior poles of the humeral head. b) glenoid axis drawn between the superior and inferior poles of the glenoid. c) both axes shown on the same slice3. d) HGCo angle formed by the axis of the glenoid and the line perpendicular to the axis of the humeral head.

Inclusion in the study required the availability of assessable antero-posterior and lateral standard radiographs and of a CT scan allowing an evaluation of the predefined study criteria. The patients meeting these criteria were divided into two groups based on clinical tolerance of the PHM. Poor clinical tolerance was defined as a UCLA Shoulder Score < 29 points and a need for surgical revision due to pain, motion-range restriction, or both. Pain was defined as a visual analogue scale score of 6 or more at rest. Pain was a criterion of poor tolerance only if accompanied with motion-range restriction. Motion-range restriction was defined as a decrease in functional amplitudes compared to the contralateral shoulder with a negative impact on daily activities. Of the 28 patients meeting these criteria, 16 had avascular necrosis of the humeral head, including 4 with a necrotic sequester. Neither patients who required revision surgery only because of hardware-related problems nor those with complex regional pain syndrome type I were eligible for inclusion in this subgroup.

Good clinical tolerance of PHM was defined as patient satisfaction with the use of the shoulder during daily activities, no requirement for revision surgery due to the PHM, and a UCLA Shoulder Score value in the good (29–33) or excellent (34–35) range (Fig. 1). Of the 18 patients meeting these criteria, 10 had avascular necrosis of the humeral head and none had a necrotic sequester.

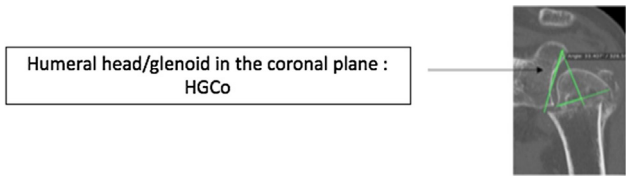

Fig. 3. Coronal plane: angle formed by the axis of the humeral head and the axis of the glenoid (HGCo) in a patient with proximal humerus malunion.

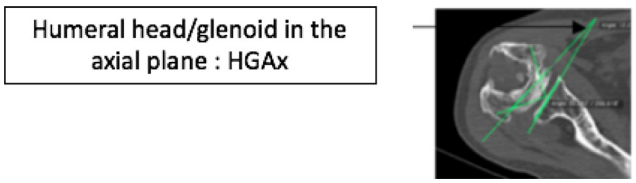

Fig. 5. Angle between the humeral head and the glenoid in the axial plane in a patient with proximal humerus malunion.

2.2. Measurement method

We measured four angles that reflect convergence or divergence of the bony structures involved in PHM, eg., the tuberosities, humeral head, glenoid, and humeral diaphysis, in the coronal and axial planes. The values of these angles reflect the amount of morphological disharmony induced by the PHM. The measurements were performed on a single CT slice in the coronal, sagittal, and axial planes. The position of the tuberosities was defined based on the centre of each tuberosity on the axial CT view. The distances between the points placed at the centres of the greater and lesser tuberosities and the centre of the glenoid (GT-G and LT-G, respectively) were measured using the OsiriX® measurement tool (Pixmeo SARL, Bernex, Switzerland).

Of the four angles, two evaluated the orientation of the humeral head (H) relative to that of the glenoid (G) in the coronal (Co) plane (HGCo) and axial (Ax) plane (HGAx) (Figs. 2–5). The angle of tuberosity divergence in the axial plane (TDAx) was measured as the angle formed by the lines connecting the centres of the tuberosities to the centre of the glenoid (Figs. 6 and 7). Finally, the orientation of the humeral head relative to the humeral diaphysis in the coronal plane was assessed based on the CCD (Fig. 2).

We used 2D multi-planar reconstruction (MPR) software to identify a reference CT slice in the coronal, sagittal, and axial planes. A standardised method was used to select these reference slices (Figs. 8 and 9). The angles were measured on anonymised digitised CT or CT-arthrography scans of the shoulder acquired with the patient supine and the arm lying along the side in neutral rotation with the elbow extended. The CT machine was a 64-row Revolution GSI (General Electric Healthcare, Chicago, IL, USA). Parameters were as follows: slice thickness, 0.625 mm; 64 barrettes, slice thickness, 0.625 mm; collimation, 40 mm; tube voltage, 120 Kv; and automatically adjusted tube current. The angles (in degrees), distances (in cm), and surface areas (in cm^2) were computed using 32-bit OsiriX® version 5.7 (Pixmeo).

2.3. Statistical analysis

Two independent senior physicians who played no role in treating the patients performed the measurements twice at an interval of 2 months. We first validated the measurement method in a control group of 30 consecutive shoulder CT scans and in a group of 46 patients with PHM. The controls had no history of shoulder injury or surgery and were free of lesions to the shoulder capsule and ligaments. We then compared the angle values between the controls and patients and between the two patient subgroups defined based on clinical tolerance of the PHM.

Descriptive statistics consisting of mean, variance, standard deviation, confidence interval, and range were computed in both the control and the patient groups. Comparisons were with the non-parametric Mann-Whitney test. Values of $P \leq 0.05$ were taken to indicate significant differences. Bland-Altman [13,14] plots were constructed to assess intra- and interobserver reproducibility. Limits of agreement of ±2 SDs were pre-defined as acceptable. The mean difference between the two values obtained by each observer was computed with the 95% confidence intervals (95%CIs). The intra-class correlation coefficient (ICC) was computed to assess intra- and interobserver correlations, as described elsewhere [15,16]. ICC values were interpreted according to Fleiss et al. [17] as follows: >0.75, excellent; 0.60–0.75, good; 0.40–0.60, fair; <0.40, poor.

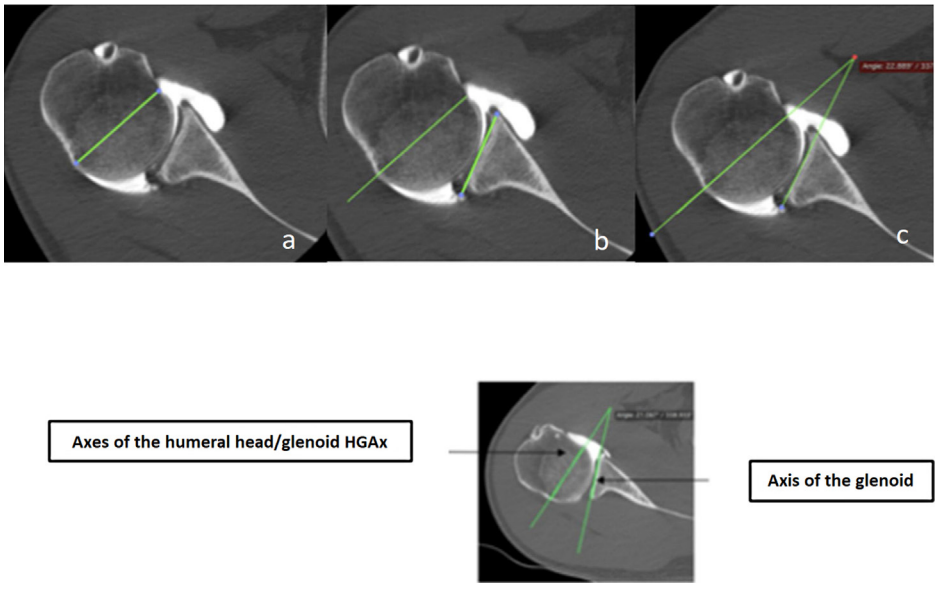

Fig. 4. Axial plane: angle formed by the axis of the humeral head and the axis of the glenoid (HGAx). a) line connecting the anterior and posterior poles of the humeral head. b) line connecting the anterior and posterior poles of the glenoid. c) measurement of the HGAx formed by the two lines.

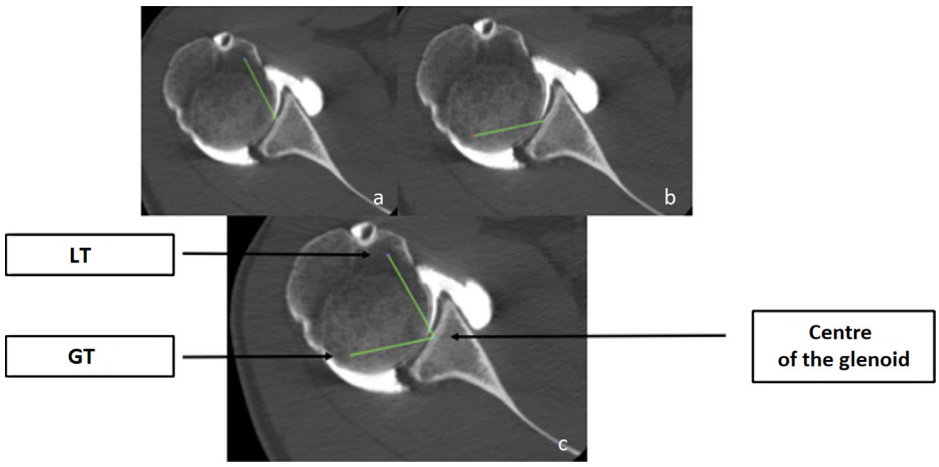

Fig. 6. Measured used to measure the angle of tuberosity divergence in the axial plane. a) distance between the centre of the lesser tuberosity (LT) and the centre of the glenoid (G). b).distance between the centre of the greater tuberosity (GT) and the centre of the glenoid. c) angle of divergence of the tuberosities formed by the intersection of the two lines.

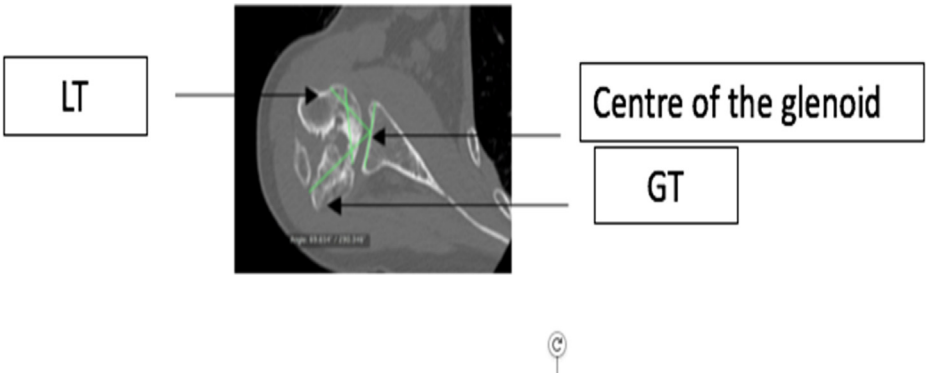

Fig. 7. Axial view in a patient with proximal humerus malunion: tuberosity divergence angle (TDAx).

The statistical analyses were performed using MedCalc software version 16.8 (Ostend, Belgium).

3. Results

3.1. Intra- and interobserver reproducibility and intraclass correlations (ICCs)

The Bland-Altman plots indicated good intra- and inter-observer reproducibility of the measurements of all four angles in both the controls and the patients (Fig. 10). Within the control group, intra- and interobserver reproducibility was best for HGCo (intra-observer 1st measurement, 95%CI, −13.9;14.4), TDAx (intraobserver 2nd measurement, 95%CI, −18.9;9.5), and HGAx (intraobserver 1st measurement, 95%CI, −2.7;1.3). Within the patient group, reproducibility was best for TDAx (interobserver 1st measurement, 95%CI, −40.6;15.3), HGAx (inter-observer 2nd measurement, 95%CI, −22.5;34.1), and HGCo (interobserver 2nd measurement, 95%CI, −38.3;26.9; intraobserver 1st measurement, 95%CI,−25.1;22) (Fig. 11).

Intraobserver ICCs were good to excellent for most angles. In the patient group, intra- and interobserver ICCs were good to excellent for HGCo and fair to excellent for TDAx. Intra- and interobserver ICCs for HGCo, HGAx, and CCD in the patients were fair to excellent (Tables 1 and 2). In both groups, GT-G and LT-G values were usually reproducible both within and between observers (Tables 1 and 2). Finally, the ICC values for selection of the reference CT slice ranged from fair to good in the control group and from fair to excellent in the patient group (Tables 1 and 2).

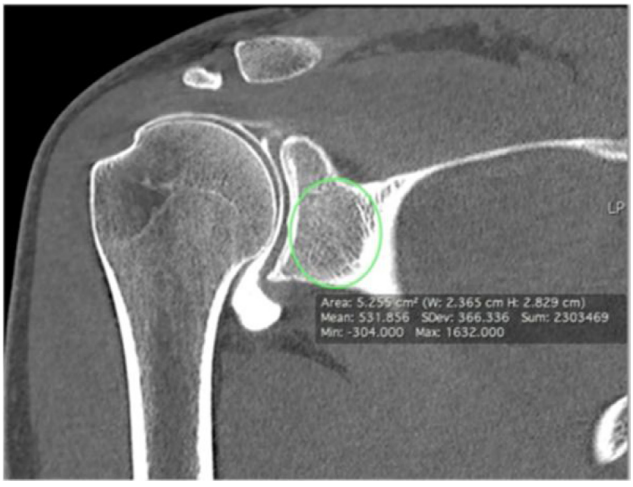

Fig. 8. First step in selecting the reference coronal computed tomography view: centring of the coronal slice just before the appearance of the coracoid notch and selection of the largest glenoid surface area (in cm^2).

3.2. Relevance of the variables

Tables 3 and 4 report the mean values of the measured distances (cm) and angles (°) and the *P* values for the comparisons between

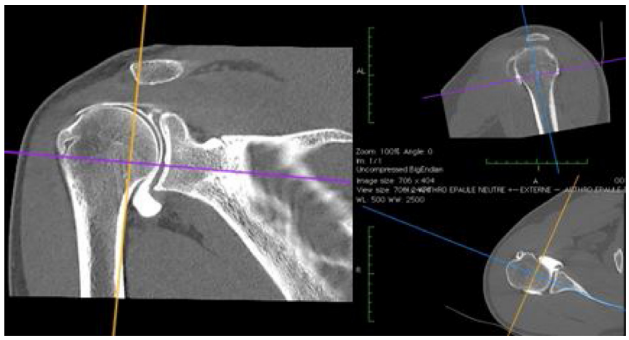

Fig. 9. Selection of the reference computed tomography views: simultaneous centring of the coronal, sagittal (axis of the shaft), and axial views; visualisation of the humeral head (H), lesser tuberosity (LT), greater tuberosity (GT), and glenoid (G).

the control and patient groups. Significant differences were found. Mean LT-G was significantly longer in the control group than in the patient group (4.01 cm [95%CI, 3.9;4.2 and 3.31 cm [95%CI, 3.2;3.4]; respectively; $P < 0.05$). The result was similar for GT-G (Table 3). Within the PHM group, the subgroup with poor tolerance had a significantly shorter mean LT-G (3.4 cm vs. 3.8 cm in the group with good tolerance) and a longer mean GT-G.

Mean TDAx was significantly greater in the patient group (72.0° vs. 56.1° in the control group, $P < 0.05$) and significantly smaller in the patients with poor tolerance (69.5° vs. 75.8° in the patients with good tolerance, $P < 0.05$). CCD, which reflects varus or valgus of the malunion, was smaller in the patients than in the controls (125.9° [95%CI, 122.9–128.9] and 129.8° [95%CI, 128.3–131.3] and significantly greater in the patient subgroup with good tolerance (131.4° vs. 122.3° in the subgroup with poor tolerance, $P = 0.007$). HGCo was significantly greater in the patients vs. the controls (66.6° vs. 52.2°, respectively) and in the patients with poor tolerance vs. those with good tolerance (70.6° vs. 60.3°, respectively; $P = 0.05$). Finally, HGAx was significantly greater in the patients than the controls (17.5° vs. 13.3°, $P = 0.55$) but was not significantly different between the two patient subgroups (17.5° vs. 16.6°).

4. Discussion

4.1. Measurement method

Our findings suggest good reproducibility and correlations for reference CT slice selection and measurements of the study angles and distances in both the control and the patient groups. In the patients, correlations were good to excellent for all four angles. In the controls, HGCo and CCD showed good reproducibility and correlations. We believe the poor interobserver correlations for HGAx and TDAx in the control group are ascribable to the absence of displacement of the humeral head and tuberosities. The use of these

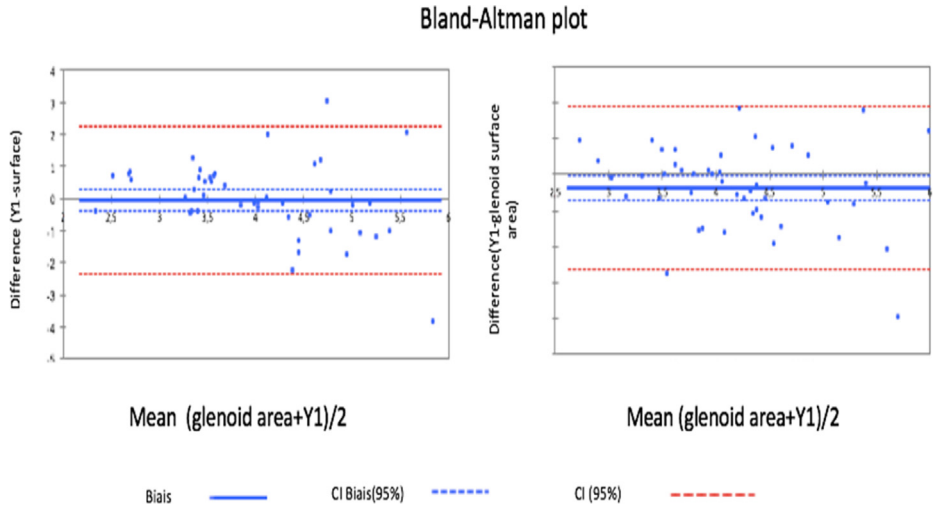

Fig. 10. Control group: Bland-Altman plot of mean intra-observer 1 and inter-observer 2 values of glenoid surface area (GSA).

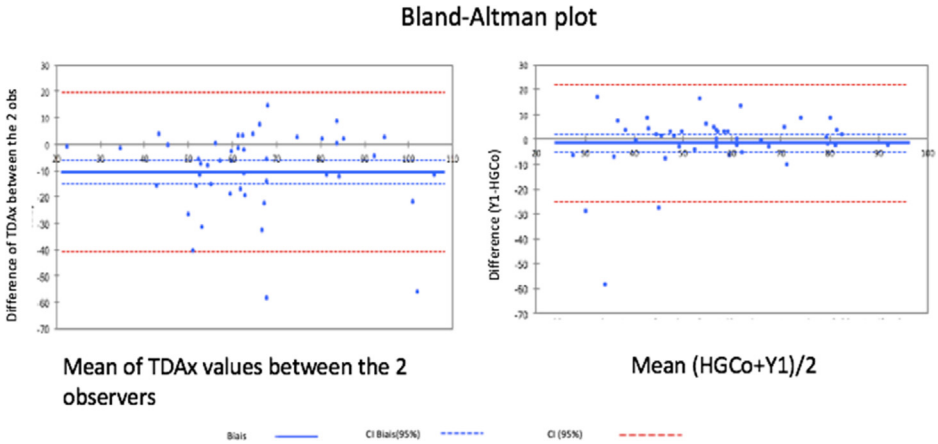

Fig. 11. Group with proximal humerus malunion: Bland-Altman plot of mean interobserver 1 TDAx values and intra-observer HGCo values. TDAx, tuberosity divergence angle in the axial plane; HGCo, angle between the humeral head and glenoid in the coronal plane.

Table 1
Intraclass correlation coefficients in the control group.

ParametersControl group	Intraobserver ICC [95%CI]		Interobserver ICC [95%CI]	
	Observer 1	Observer 2	Observer 1	Observer 2
HGAx	0.8 [0.5–0.9]	0.8 [0.3–0.9]	0.1 [−0.1–0.3]	0.1 [0.7−0.5]
Category	Excellent	Excellent	Poor	Poor
TDAx	0.3 [−0.4–0.6]	0.48 [−0.04–0.7]	−0.07 [−0.4–0.3]	0.03 [−0.1–0.1]
Category	Poor	Fair	Poor	Poor
LT-G	0.7 [0.4–0.8]	0.9 [0.8–0.9]	0.8 [0.5–0.9]	0.9 [0.8–0.9]
Category	Good	Excellent	Excellent	Excellent
GT-G	0.5 [0.04–0.7]	0.9 [0.7−0.9]	0.4 [−0.2–0.7]	0.4 [−0.1–0.7]
Category	Fair	Excellent	Fair	Fair
HGCo	0.9 [0.7–0.9]	0.94 [0.8–0.9]	0.9 [0.8–0.9]	0.9 [0.8–0.9]
Category	Excellent	Excellent	Excellent	Excellent
CCD	0.9 [0.8–0.9]	0.7 [0.4–0.8]	0.8 [0.5–0.9]	0.9 [0.8–0.9]
Category	Excellent	Good	Excellent	Excellent

95%CI; 95% confidence interval; HGAx; angle formed by the axis of the humeral head and the axis of the glenoid in the axial plane; TDAx; angle of divergence of the tuberosities in the axial plane; LT-G; distance from the centre of the lesser tuberosity to the centre of the glenoid; GT-G; distance from the centre of the greater tuberosity to the centre of the glenoid; HGCo; angle formed by the perpendicular to the axis of the humeral head and the axis of the glenoid in the coronal plane; CCD; centrum collum diaphyseal angle.

Table 2
Intraclass correlation coefficients in the group with proximal humerus malunion.

ParametersPHM group	Intraobserver ICC [95%CI]		Interobserver ICC [95%CI]	
	Observer 1	Observer 2	Observer 1	Observer 2
HGAx	0.8 [0.6;0.8]	0.9 [0.9;0.9]	0.7 [0.6;0.8]	0.9 [0.9;0.9]
Category	Excellent	Excellent	Excellent	Excellent
TDAx	0.5 [;0.2;0.7]	0.8 [0.7;0.9]	0.7 [0.3;0.8]	0.5 [0.3;0.7]
Category	Fair	Excellent	Excellent	Fair
LT-G	0.6 [0.4;0.6]	0.8 [0.7;0.9]	0.6 [0.4;0.8]	0.8 [0.7;0.9]
Category	Good	Excellent	Good	Excellent
GT-G	0.5 [0.1;0.7]	0.9 [0.8;0.9]	0.4 [0.2;0.7]	0.4 [0.1;0.7]
Category	Fair	Excellent	Fair	Fair
HGCo	0.6 [0.4;0.8]	0.9 [0.8;0.9]	0.6 [0.6;0.8]	0.7 [0.5;0.8]
Category	Good	Excellent	Good	Good
CCD	0.9 [0.9;1]	0.9 [0.8;0.9]	0.9 [0.9;1]	0.9 [0.9;1]
Category	Excellent	Excellent	Excellent	Excellent

PHM; proximal humerus malunion; 95%CI; 95% confidence interval; HGAx; angle formed by the axis of the humeral head and the axis of the glenoid in the axial plane; TDAx; angle of divergence of the tuberosities in the axial plane; LT-G; distance from the centre of the lesser tuberosity to the centre of the glenoid; GT-G; distance from the centre of the greater tuberosity to the centre of the glenoid; HGCo; angle formed by the perpendicular to the axis of the humeral head and the axis of the glenoid in the coronal plane; CCD; centrum collum diaphyseal angle.

Table 3
Values of each study variable in the control group.

VariablesControl group	HGAx	HGCo	TDAx	CCD	LT-G	GT-G
Mean	13.8	52.2	56.1	129.8	4.0	4.7
SD	6.1	11.3	6.5	5.8	0.6	0.6
Variance	37.2	202.6	43.1	34.2	0.3	0.3
95%CI	11.8;14.9	49.4;55.1	54.45;57.8	128.3;131.3	3.9;4.2	4.6;4.7
Minimum	5.7	27.5	39.9	112.6	2.5	3.17
Maximum	70.7	74.1	78.2	141.3	5.2	6.1

95%CI; 95% confidence interval; HGAx; angle formed by the axis of the humeral head and the axis of the glenoid in the axial plane; HGCo; angle formed by the perpendicular to the axis of the humeral head and the axis of the glenoid in the coronal plane; TDAx, angle of divergence of the tuberosities in the axial plane; CCD; centrum collum diaphyseal angle; LT-G, distance from the centre of the lesser tuberosity to the centre of the glenoid; GT-G; distance from the centre of the greater tuberosity to the centre of the glenoid.

Table 4
Values of each study variable in the group with proximal humerus malunion.

Variables Group with PHM	HGAx	HGCo	TDAx	CCD	LT-G	GT-G
Mean	17.0	66.6	72.0	125.9	3.3	3.6
SD	11.0	17.7	20.8	15	0.7	0.8
Variance	121.8	313.4	435.6	224.8	0.4	0.6
95%CI	14.8–19.3	63–70.2	67.8–76.3	122.9–128.9	3.2–3.4	3.5–3.8
Minimum	3.5	29.8	2.7	82.2	1.2	1.5
Maximum	56.9	107.5	130.4	154.2	5.2	6.4

PHM; proximal humerus malunion; 95%CI; 95% confidence interval; HGAx; angle formed by the axis of the humeral head and the axis of the glenoid in the axial plane; HGCo; angle formed by the perpendicular to the axis of the humeral head and the axis of the glenoid in the coronal plane; TDAx; angle of divergence of the tuberosities in the axial plane; CCD; centrum collum diaphyseal angle; LT-G; distance from the centre of the lesser tuberosity to the centre of the glenoid; GT-G; distance from the centre of the greater tuberosity to the centre of the glenoid.

Table 5
Comparison of the mean study parameter values between the group with proximal humerus malunion and the control group.

	Control group	PHM group	*P* value
TDAx	56.1	72.0	< 0.05
CCD	129.8	125.9	0.16
HGCo	52.2	66.6	< 0.05
HGAx	13.8	17.0	0.01
LT-G	4.01	3.55	< 0.05
GT-G	4.71	4.23	0.53

PHM; proximal humerus malunion; TDAx; angle of divergence of the tuberosities in the axial plane; CCD; centrum collum diaphyseal angle; HGCo; angle formed by the perpendicular to the axis of the humeral head and the axis of the glenoid in the coronal plane; HGAx; angle formed by the perpendicular to the axis of the humeral head and the axis of the glenoid in the axial plane; LT-G; distance from the centre of the lesser tuberosity to the centre of the glenoid; GT-G; distance from the centre of the greater tuberosity to the centre of the glenoid.

two angles is appropriate only if the head and tuberosities are significantly displaced.

Budge et al. [18] used the plane of the scapula as the reference for 3D reconstructions to correct for bias related to shoulder position during CT image acquisition. Nevertheless, individual anatomical variations are not eliminated by this method.

In the patient group, non-reproducible (outlier) HGCo values were found in 2 patients with non-spherical humeral heads due to avascular necrosis. Positioning the reference points on the humeral head may be less accurate in this situation.

Our measurement technique had a short learning curve and was reliable in the group of patients with PHM.

4.2. Relevance of the variables

The significant shortening of LT-G and GT-G in the group with PHM compared to the controls reflected impaction or necrosis of the humeral head during fracture healing. LT-G was significantly shorter in the patients with poor tolerance, indicating medialisation of the lesser tuberosity and posterior healing of the greater tuberosity on the axial views. These anatomical changes were quantified in our study.

The TDAx, a marker of tuberosity divergence, was greater in the patients than in the controls. This difference is ascribable to posterior displacement of the greater tuberosity by the infraspinatus and medialisation of the lesser tuberosity by the sub-scapularis during fracture healing. It was consistent with the shorter LT-G and GT-G distances in the group with PHM.

By using a fixed axial reference point (the centre of the glenoid), we were able to demonstrate and quantify the mean values of the anatomical changes. The smaller TDAx in the patients with poorly tolerated vs. well tolerated PHM is ascribable to inferior and medial displacement of the lesser tuberosity and/or to posterior displacement of the greater tuberosity [2]. The TDAx value reflects the relative positions of the two tuberosities and therefore confirms malposition of the tuberosities as a PHM criterion. Malposition of the greater tuberosity had been reported previously [18,19] but had not been evaluated relative to the position of the lesser tuberosity in the axial plane. The TDAx value can be correlated with the clinical tolerance of PHM. The greater the retraction of the tuberosities, the smaller the TDAx value. The insertion of the supraspinatus and subscapularis tendons into the greater and lesser tuberosities, respectively, explain that the functional limitation was poorly tolerated when the TDAx value exceeded 70° in our patients with PHM.

The greater values of the HGAx and HGCo in the PHM group compared to the control group constitute objective evidence of a

Fig. 12. Decrease in the surface area of contact between the humeral and glenoid cartilage surfaces with a decrease in the HGCo angle.

Fig. 13. Correlation between a smaller TDAx angle and clinical tolerance of the proximal humerus malunion.

decrease in the surface area of glenohumeral joint contact, with tilting of the humeral head inferiorly in the coronal plane and posteriorly in the axial plane. The increase in the HGCo value was thus related to a decrease in the surface area of contact between the humeral head and the glenoid (Fig. 12). PHM tolerance was directly related to the decrease in the HGCo value. The biomechanical corollary of this decrease in contact surface area is restriction of the gliding surface of the gleno-humeral joint. PHM tolerance seemed to remain good as long as HGCo was no greater than 60°.

We were thus able to quantify PHM disharmony: tuberosity divergence with a TDAx > 70°, HGAx > 16°, HGCo > 60°, and LT-G < 4 cm defined PHM. Our data suggest that poor PHM tolerance occurred when TDAx was < 70°, HGCo was > 65°, and CDD was < 125° (Fig. 13).

We used CT views in two planes to assess malposition of the bony components of PHM, namely, the tuberosities, the humeral head, and the glenoid. When combined with radiographs, the CT measurements provide greater accuracy with less underestimation of the relative positions of the bony components in the three planes. No other similar studies are available for comparison to the mean values obtained in our study. CT has been validated for assessing claims related to PHM. Guidelines for pre-operative 3D planning of corrective osteotomies performed using patient-specific guides have been developed [19].

Table 6
Comparison of the mean study parameter values between the subgroup with poorly tolerated malunion and the subgroup with well tolerated malunion.

PHM	Poor tolerance	Good tolerance	*P* value
AOT	69.5	75.8	0.05
CCD	122.3	131.4	0.007
TGF	70.6	60.3	0.05
TGA	17.5	16.6	1.17
TMING	3.4	3.7	0.05
TMAJG	4.1	4.3	0.2

PHM; proximal humerus malunion; TDAx; angle of divergence of the tuberosities in the axial plane; CCD, centrum collum diaphyseal angle; HGCo; angle formed by the perpendicular to the axis of the humeral head and the axis of the glenoid in the coronal plane; HGAx; angle formed by the perpendicular to the axis of the humeral head and the axis of the glenoid in the axial plane; LT-G; distance from the centre of the lesser tuberosity to the centre of the glenoid; GT-G; distance from the centre of the greater tuberosity to the centre of the glenoid.

Our study confirms the good reproducibility and reliability of the measurements used, as well as their relevance, as we were able to identify angle cut-offs for differentiating patients with PHM from controls and, among the patients, those with good vs. poor tolerance of the PHM. The results confirm the reliability of the study measurements performed on CT views of shoulders with PHM. The learning curve of the measurement technique was short. We believe that the CT measurements must be used in combination with clinical data. The CT measurements provide an evaluation of the relative positions of the bony structures of the shoulder with postfracture sequelae. We have described objective, reliable, and reproducible criteria for bony malposition that correlate with anatomical and clinical findings. The angles described could be used to develop a score with cut-offs for predicting poor clinical tolerance. Such a score might prove helpful in a prospective study comparing homogeneous groups of patients with PHM.

4.3. Study limitations

Our study has a number of sources of bias, notably regarding the positioning of the reference points used to determine the angles and distances. Positioning of the reference point on the glenoid used to measure TDAx, LT-G, and GT-G is subjective. Before starting the study, we evaluated the importance of this source of bias by assessing the reproducibility of reference point placement by three different observers. Each observer determined the centres of the lesser tuberosity, greater tuberosity, and glenoid on three separate occasions several days apart. The points were then transferred to a 3D reconstruction. Only minimal differences in point position were found. Our CT slice selection and measurement technique was therefore deemed reliable.

Rotation of the arm during image acquisition can lead to variations in measured values. All CT images were acquired with the patient supine and the arm along the body in neutral rotation with the elbow extended. We found no other means of limiting this source of bias.

Greater measurement variability was seen in the patients with humeral head necrosis, as the loss of head sphericity combined with impaction of the head and tuberosities altered the anatomical relationships. It seems reasonable to assume that tuberosity position is less reliably determined in patients with avascular necrosis. Non-reproducible (outlier) values of HGCo were seen in only 2 patients, both of whom had avascular necrosis.

The CCD angle is a well-established parameter measured on radiographs to assess the amount of valgus or varus of PHM. In our study, the CCD was measured on CT views to further assess the PHM in the coronal plane. PHM with varus deformity has been previously reported to be associated with poorer clinical tolerance [2,4,7]. In keeping with these data, CCD was smaller in our patient subgroup with poor tolerance compared to the subgroup with good tolerance (Table 5). Of the patients with PHM, 14 had a varus deformity, a finding that may explain the significant CCD difference between the PHM and control groups. Of the 14 patients with varus PHM, 12 (12/28) had poor tolerance and only 2 (2/18) good tolerance. The lack of homogeneity of the two PHM subgroups influenced the CCD results (Table 6). The CCD should be evaluated in combination with the other parameters used in this study.

The angles used for this study were determined on 2D reconstructions. We were unable to find a means of establishing the correlations in 3D.

5. Conclusion

The angles that we deem indispensable to a CT evaluation of PHM tolerance are TDAx, HGCo, and HGAx. TDAx reflects divergence of the tuberosities in the axial plane due to retraction of the tuberosities and functional retraction of the rotator cuff. The HGCo and HGAx angles reflect the surface area of gleno-humeral cartilage contact in the coronal and axial planes, respectively.

The TDAx, HGCo, HGAx, and CCD angles are relevant and reproducible parameters for the CT evaluation of PHM. The method described here was reproducible and reliable in both the controls and the patients with PHM. The CT findings correlate with anatomical alterations that we were able to model in two dimensions.

Disclosure of interest

The authors declare that they have no competing interest.

Funding

None.

Contributions

AG and BC: performed the study and wrote the manuscript.
PJM and JA: wrote the manuscript.
CL and MC: revised the manuscript.

References

[1] Palvanen M, Kannus P, Niemi S, Parkkari J. Update in the epidemiology of proximal humeral fractures. Clin Orthop 2006;442:87–92.
[2] Duparc F. Malunion of the proximal humerus. Orthop Traumatol Surg Res OTSR 2013;99:S1–11.
[3] Boileau P, Trojani C, Walch G, Krishnan SG, Romeo A, Sinnerton R. Shoulder arthroplasty for the treatment of the sequelae of fractures of the proximal humerus. J Shoulder Elbow Surg 2001;10:299–308.
[4] Mansat P, Bonnevialle N. Treatment of fracture sequelae of the proximal humerus: anatomical vs reverse shoulder prosthesis. Int Orthop 2015;39:349–54.
[5] Siegel JA, Dines DM. Proximal humerus malunions. Orthop Clin North Am 2000;31:35–50.
[6] Mansat P, Guity MR, Bellumore Y, Mansat M. Shoulder arthroplasty for late sequelae of proximal humeral fractures. J Shoulder Elbow Surg 2004;13:305–12.
[7] Moineau G, McClelland WB, Trojani C, Rumian A, Walch G, Boileau P. Prognostic factors and limitations of anatomic shoulder arthroplasty for the treatment of posttraumatic cephalic collapse or necrosis (type-1 proximal humeral fracture sequelae). J Bone Joint Surg Am 2012;94:2186–94.
[8] Beredjiklian PK, Iannotti JP, Norris TR, Williams GR. Operative treatment of malunion of a fracture of the proximal aspect of the humerus. J Bone Joint Surg Am 1998;80:1484–97.
[9] Boileau P, Chuinard C, Le Huec J-C, Walch G, Trojani C. Proximal humerus fracture sequelae: impact of a new radiographic classification on arthroplasty. Clin Orthop 2006;442:121–30.
[10] Doornberg J, Lindenhovius A, Kloen P, van Dijk CN, Zurakowski D, Ring D. Two and three-dimensional computed tomography for the classification and management of distal humeral fractures. Evaluation of reliability and diagnostic accuracy. J Bone Joint Surg Am 2006;88:1795–801.

[11] Vlachopoulos L, Schweizer A, Meyer DC, Gerber C, Fürnstahl P. Three-dimensional corrective osteotomies of complex malunited humeral fractures using patient-specific guides. J Shoulder Elbow Surg 2016;25:2040–7.
[12] Friedman RJ, Hawthorne KB, Genez BM. The use of computerized tomography in the measurement of glenoid version. J Bone Joint Surg Am 1992;74:1032–7.
[13] Bland JM, Altman DG. Statistical methods for assessing agreement between two methods of clinical measurement. Lancet Lond Engl 1986;1:307–10.
[14] Bland JM, Altman DG. Agreement between methods of measurement with multiple observations per individual. J Biopharm Stat 2007;17:571–82.
[15] Lee J, Koh D, Ong CN. Statistical evaluation of agreement between two methods for measuring a quantitative variable. Comput Biol Med 1989;19:61–70.
[16] Romero Morales C, Calvo Lobo C, Rodríguez Sanz D, Sanz Corbalán I, Ruiz Ruiz B, López López D. The concurrent validity reliability of the Leg Motion system for measuring ankle dorsiflexion range of motion in older adults. Peer J 2017;5:e2820.
[17] Shrout PE, Fleiss JL. Intraclass correlations: uses in assessing rater reliability. Psychol Bull 1979;86:420–8.
[18] Budge MD, Lewis GS, Schaefer E, Coquia S, Flemming DJ, Armstrong AD. Comparison of standard two-dimensional and three-dimensional corrected glenoid version measurements. J Shoulder Elbow Surg 2011;20:577–83.
[19] Vlachopoulos L, Schweizer A, Meyer DC, Gerber C, Fürnstahl P. Three-dimensional corrective osteotomies of complex malunited humeral fractures using patient-specific guides. J Shoulder Elbow Surg [Internet]. [cited 2016 Aug 17]; Available from: http://www.sciencedirect.com/science/article/pii/S1058274616301549.